GRØNLANDS GEOLOGISKE UNDERSØGELSE
Bulletin No. 135

Metasomatic zonation of an ultramafic lens at Ikátoq, near Færingehavn, southern West Greenland

by

Martin R. Sharpe

KØBENHAVN 1980

Grønlands Geologiske Undersøgelse

(The Geological Survey of Greenland)

Øster Voldgade 10, DK-1350 Copenhagen K

Bulletins

No. 121 Early Silurian (Late Llandovery) rugose corals from western North Greenland. 1977 *by* R. A. McLean. D.kr. 46.00

No. 122 Gardiner intrusion, an ultramafic complex at Kangerdlugssuaq, East Greenland. 1977 *by* W. Frisch & H. Keusen. D.kr. 80.00

No. 123 Stratigraphy, tectonics and palaeogeography of the Jurassic sediments of the areas north of Kong Oscars Fjord, East Greenland. 1977 *by* F. Surlyk. D.kr. 50.00

No. 124 The Fiskenæsset complex. West Greenland Part III Chemistry of silicate and oxide minerals from oxide-bearing rocks, mostly from Qeqertarssuatsiaq. 1977 *by* I. M. Steele, F. C. Bishop, J. V. Smith & B. F. Windley. D.kr. 27.00

No. 125 Petrology of the late lavas of the Eriksfjord Formation, Gardar province, South Greenland. 1977 *by* J. Gutzon Larsen. D.kr. 25.00

No. 126 Cuprostibite and associated minerals from the Ilímaussaq intrusion, South Greenland, 1978 *by* S. Karup-Møller, L. Løkkegaard, E. I. Semenov & H. Sørensen. D.kr. 55.00

No. 127 The ore minerals of the Ilímaussaq intrusion: their mode of occurrence and their conditions of formation. 1978 *by* S. Karup-Møller. D.kr. 58.00

No. 128 Submarine fan sedimentation along fault scarps on tilted fault blocks (Jurassic-Cretaceous boundary, East Greenland). 1978 *by* F. Surlyk. D.kr. 125.00

No. 129 Holocene stratigraphy and vegetation history in the Scoresby Sund area, East Greenland. 1978 *by* S. Funder. D.kr. 95.00

No. 130 Organic compounds from Cretaceous coals of Nûgssuaq, West Greenland. 1978 *by* J. Lam & K. R. Pedersen. D.kr. 23.00

No. 131 Llandovery trilobites from Washington Land, North Greenland. 1979 *by* P. D. Lane. D.kr. 65.00

No. 132 Dinoflagellate cysts and acritarchs from the Middle and Upper Jurassic of Jameson Land, East Greenland. 1979 *by* R. A. Fensome. D.kr. 140.00

No. 133 The petrology and age of alkaline mafic lavas from the nunatak zone of central East Greenland. 1979 *by* C. K. Brooks, A. K. Pedersen & D. C. Rex. D.kr. 50.00

No. 134 Acritarchs from the Upper Proterozoic and Lower Cambrian of East Greenland. 1979 *by* G. Vidal. D.kr. 65.00

No. 135 Metasomatic zonation of an ultramafic lens at Ikátoq, near Færingehavn, southern West Greenland. 1980 *by* M. R. Sharpe.

Bulletins up to no. 114 were also issued as parts of *Meddelelser om Grønland*, and are available from Nyt Nordisk Forlag – Arnold Busck, Købmagergade 49, DK–1150 Copenhagen K, Denmark.

GRØNLANDS GEOLOGISKE UNDERSØGELSE
Bulletin No. 135

Metasomatic zonation of an ultramafic lens at Ikátoq, near Færingehavn, southern West Greenland

by

Martin R. Sharpe

1980

Abstract

The Ikátoq zoned ultramafic lens occurs as an elliptical body in Archaean gneisses and amphibolites to the south of Færingehavn, southern West Greenland. From the unaltered serpentinite core to the contact with the surrounding gneisses five zones were distinguished: serpentinite (5), talc-carbonate rock (4), talc (3), amphibole (2) and chlorite (1): their interrelationships are discussed in the light of the theory of zoning. It is shown that these five main lithological types developed from a common parent rock under the influence of low temperature metamorphism as a process of steatisation – the outer chlorite zone representing altered host rocks, whilst the inner talc, talc-carbonate and serpentinite shells represent changed serpentine core. The original junction between the two parent rocks lies in the amphibole zone.

The growth process of the zones is discussed and evidence concerning these mechanisms is presented.

Estimates of bulk transport and ion migration during the alteration are developed from the chemical analyses, based on whole-rock formulas and equivalent volumes, using ideal-mineral reaction stoichiometry. The system was open to migrating components, and it is shown that the body lost Mg to the gneisses, which in turn supplied some Ca and K to the reacting system. It is likely that CO_2 and H_2O were permanently in excess.

A volume contraction of approximately 6 per cent during the steatisation process is postulated.

Author's address:
Institute for Geological Research on the Bushveld Complex
University of Pretoria
Hillcrest
Pretoria 0083
Republic of South Africa

Contents

Introduction 5
Lithological descriptions 5
Gneisses 5
Chlorite (zone 1) 7
Amphibole (zone 2) 8
Talc (zone 3) 12
Talc-carbonate (zone 4) 12
Serpentinite (zone 5) 12
Veins 13
Rock Chemistry 14
Gneisses 14
Ultramafic lens 14
Variations across the contact between lens and gneiss 16
Quantitative estimations of ion migration 18
Zonal geochemistry 23
Gneiss → chlorite zone alteration 23
Chlorite → amphibole zone alteration 26
Amphibole → talc zone alteration 27
Talc → talc-carbonate zone alteration 28
Serpentinite → talc-carbonate zone alteration 28
Discussion 28
Conclusions 29
Acknowledgements 30
References 30

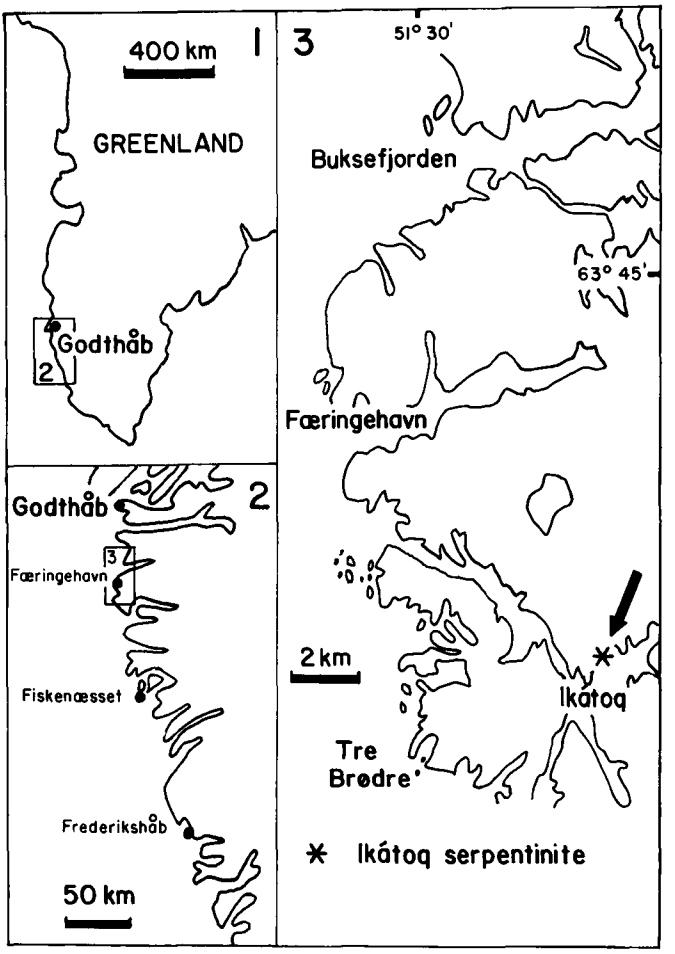

Fig. 1. Map to show the location of the Ikátoq zoned ultramafic lens.

Introduction

A zoned ultramafic lens, originally described by Windley (1972), 35 × 6 m in size, occurs as a concordant ellipsoid with faulted contacts within Precambrian gneisses in Ikátoq, to the south of Færingehavn, southern West Greenland (fig. 1). It is not cut by either representatives of the Nûk gneisses (2850 m.y.) or the Qôrqut granite (2600 m.y.) – (Moorbath & Pankhurst, 1976). The lower age bracket, however, is unproven because Qôrqut granite material is uncommon in this area.

The zoning in the lens comprises five major concentric shells of differing mineralogy, which from the centre to the margin of the lens contain dominant serpentine, talc and carbonate, talc, amphibole, and chlorite. Subzones are developed within each of these major divisions (figs 2 & 3). The surrounding gneiss envelope was considerably affected by metasomatism related to the steatisation (used in the sense of Chidester, 1962); the effects of this alteration are detectable up to 100 m from the lens across the strike.

The enveloping gneisses form part of the early Archaean craton and were involved in their last major metamorphic event *c.* 2850 m.y. ago (Black *et al.*, 1973) during which the pressure temperature regime has been estimated as being approximately 7.5 kb at 750°C in this region (Wells, 1976).

The subzone compositions were determined by microscopic examination of thin sections, bulk rock analyses (XRFS) and X-ray diffraction (XRD). These data were used to estimate the amount of bulk transport and the change in volume of the lens.

Lithological descriptions

Gneisses

The envelope comprises predominantly Nûk material with thin intercalated amphibolite strips which may represent Malene supracrustals (McGregor, 1973). This gneiss melange surrounding the lens is unaltered at distance, but the growth of secondary minerals during serpentinisation and steatisation has drastically changed the nature of the gneisses close to the ultramafic lens. Alteration first becomes noticeable about 50 to 100 m from the contact, with the development of clinozoisite mosaics in the plagioclase. Alteration intensifies laterally with the gradual replacement of biotite by chlorite together with an increase in the amount of modal K-feldspar. Blocky clinozoisite growth and sericitisation of the plagio-

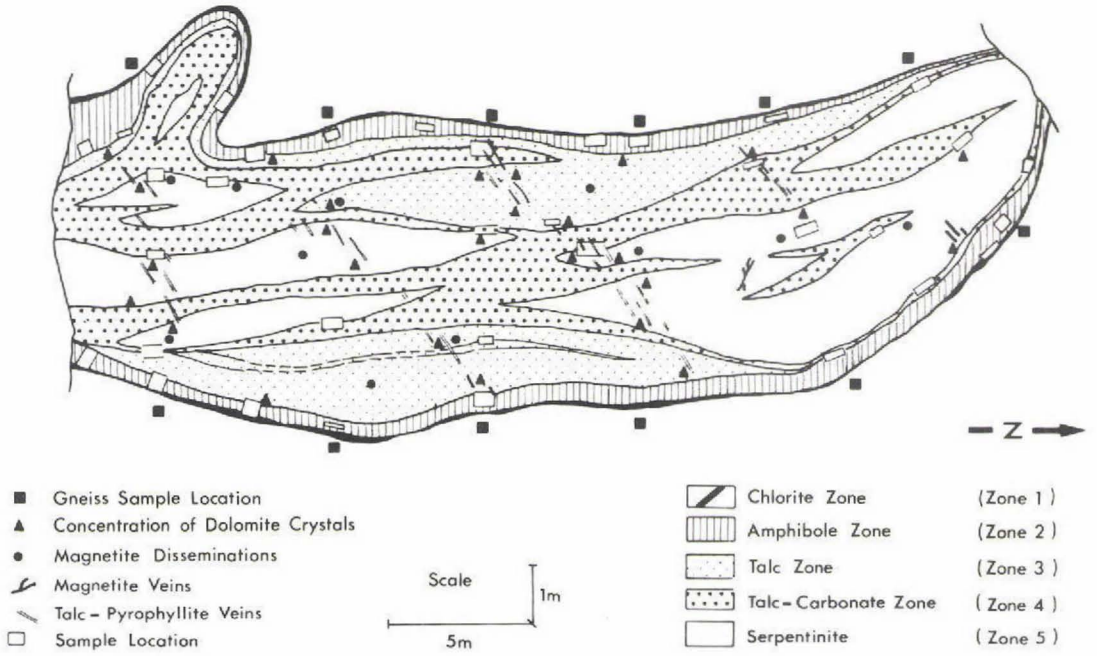

Fig. 2. Map of the Ikátoq zoned ultramafic lens showing the disposition of the zones and sample positions.

clase also occurs concomitantly. At the contact between the gneiss envelope and the ultramafic lens, the plagioclase is mostly changed to clinozoisite, relict grains selectively developing albitic rims and disrupting the gneiss fabric. Traces of ilmenite, sphene, allanite, rutile, apatite and zircon are present in the gneisses, but die out rapidly into the lens itself.

Chlorite (zone 1)

This layer is between two and 200 mm thick and occurs at the contact between the lens and the host gneisses. It typically consists of chlorite (95 to 100 per cent) with traces of hornblende, sphene, rutile, apatite, talc and zircon and may contain thin strips of talc- or amphibole-rich material. This zone cuts into the albite- and clinozoisite-rich gneisses, leaving isolated pockets with concentrations of non-reactive ilmenite, zircon or apatite. Kink-bands are developed where the cleavage of the chlorite is not aligned parallel to the gneiss-chlorite zone boundary. The chlorite is predominantly sheridanite, but other micas such as pyrophyllite and rare chlorites of composition intermediate between these two extremes occur, as shown by XRD. There is no systematic spatial distribution of these minerals.

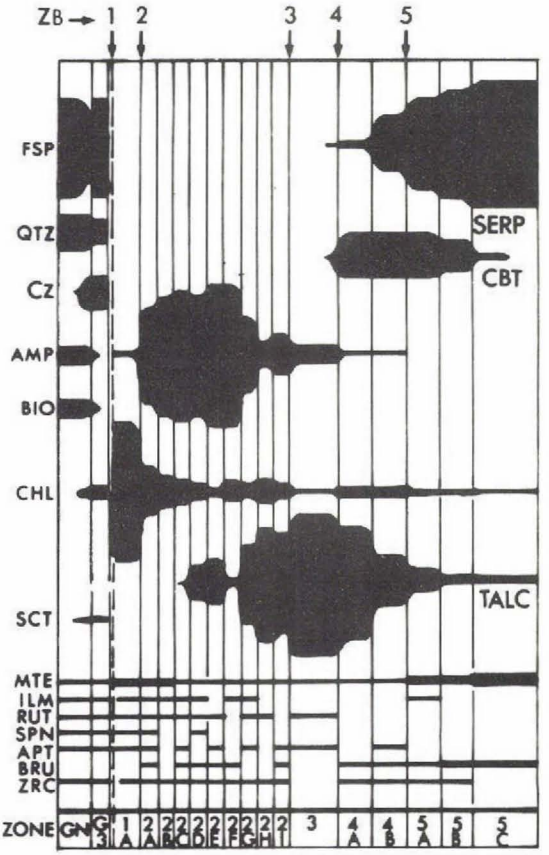

Fig. 3. Variation diagram to show the mineralogical differences between the various subzones. Abbreviations as in table 1 plus: Rut = rutile, Spn = sphene, Apt = apatite, Bru = brucite, Zrc = zircon.

Amphibole (zone 2)

The chlorite zone is digested and replaced on the inside margins by the amphibole zone, which may reach one metre in thickness, along the sharply-defined (2–3 mm) zone boundary (ZB) 2 (fig. 4). Nine subzones have been defined (2A to 2I, table 1) by differing proportions of actinolite, tremolite, hornblende, talc, carbonate (dolomite to magnesite), chlorite and serpentine, but generally these subzones are not all found in a single traverse across the zone. Subzone 2A consists of a layer of hornblende, actinolite and chlorite with relict sphene, apatite and zircon; it forms a permanent buffer between zones 1 and 2. Subzones 2B to 2I occur as elongate strips and make up the majority of zone 2. The distinctive subzone 2D consists of radiating bundles of dendritic, acicular actinolite crystals up to 160 mm long, which are replaced at their inner terminations by talc (fig. 5).

Both the fern-like protuberances (fig. 6) and the thin probes of amphibole (fig.

Table 1. Modal compositions and dimensions of the zones in the Ikátoq ultramafic lens

		Mode (vol. %)													
Subzone	F	Chl	Hbl	Trem Act	Talc	Cbt	Serp	Mte Ilm	Accs	Plag	Qtz	Bio	Mus Sct	Cz	Zone width (m)
1A	1.00	95	x	o	o	o	o	x	x					x	
1B		5		x	73	15	o	5	o					o	0.05
1C		x		95	o			o	x					o	
1D		55				o		42	2						
---															ZB2
2A	0.05	32	45	15	x	o	o	5	x						
2B	0.10	21	x	75	x	x	o	5	x						
2C	0.05	14	o	80	o	o	o	4	x						
2D	0.25	10		60	20	5	x	2	2						
2E	0.05	5	o	60	24	10	o	x	o						0.35
2F	0.05	13		85	x	o	o	x	o						
2G	0.10	10		42	45	x	o	2	o						
2H	0.05	15	o	16	65	2	o	2	o						
2I	0.30	12		24	60	x	3	x	o						
---															ZB3
3	1.00	x		10	85	o	3	2	o						0.60
---															ZB4
4A	0.50	5		x	63	25	5	x	o						
4B	0.50	5		o	29	24	36	5	o						0.70
---															ZB5
5A	0.20	x			15	25	54	5	o						
5B	0.30	2			5	18	65	5	5						1.30
5C	0.50	2			5	5	75	10	3						
		Mean modes of all shells including gneisses													
ON			8			o		1	1	60	20	8	1	1	20.00
BN		4	2	o				1	1	56	15	2	4	5	0.05
1		92		5	o	o	o	3							0.05
2		15		70	10	3	o	2							0.35
3		3		5	90	o	o	2							0.60
4		o		o	53	40	5	2							0.70
5		o		o	5	10	80	5							1.30

Abbreviations: Chl=chlorite, Hbl=hornblende, Trem=tremolite, Act=actinolite, Cbt=carbonate, Serp=serpentine, Mte=magnetite, Ilm=ilmenite, Accs=rutile + zircon + apatite + chromite, Plag=plagioclase, Qtz=quartz, Bio=biotite, Mus=muscovite, Sct=sericite, Cz=clinozoisite; ON=outside gneiss, BN=bordering gneiss; F=relative width of subzone. x=>1 per cent and o=<1 per cent in the mode.

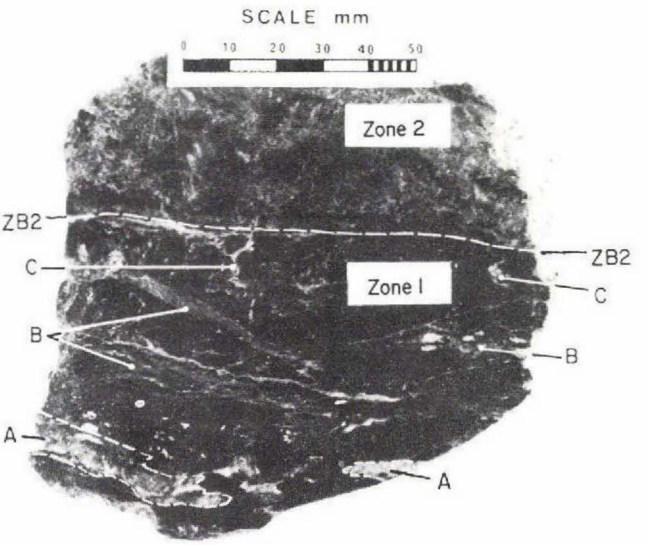

Fig. 4. A specimen from the chlorite zone showing rare inclusions of albite-porphyroblast rock (A) in the chlorite at the 'base' of the sample and the sharp ZB2 transition to the amphibole zone. Thin, discordant veins (B) are talc-carbonate rock which cut the chlorite zone. Impersistent, pale-coloured migration channels (C) cut the sample.

7) were mechanisms by which zone 2 cut into zone 1. They are both keyed upon the concept of migration channels, which are regions of vein-like, fine-grained material which the metasomatic fluids may have used as pathways through the relatively impermeable chlorite shell and which the amphiboles used as a locus for growth. Figure 8 shows an illustration of typical features of the amphibole zone, diagrammatically incorporating these phenomena.

Talc (zone 3)

The boundary between the amphibole and talc shells, ZB3, is sharp, and migrated outwards by gradual 'talcisation' of zone 2. The talc shell (steatite of Chidester, 1962; Jahns, 1967) forms a 0.2 to 0.5 m layer between the talc-carbonate and amphibole shells. Talc forms more than 90 per cent of the rock, magnetite is ubiquitous and amphibole, serpentine and carbonate are present. A faint, rare banding which may have been inherited from the layering in the serpentinite, was preserved through the steatisation process.

Talc-carbonate (zone 4)

The boundary between the talc and talc-carbonate zones, ZB4, is not sharply-defined because tongues of carbonate-bearing material project into the talc zone and disrupt the contact (fig. 2). These lobate channels also penetrate into the

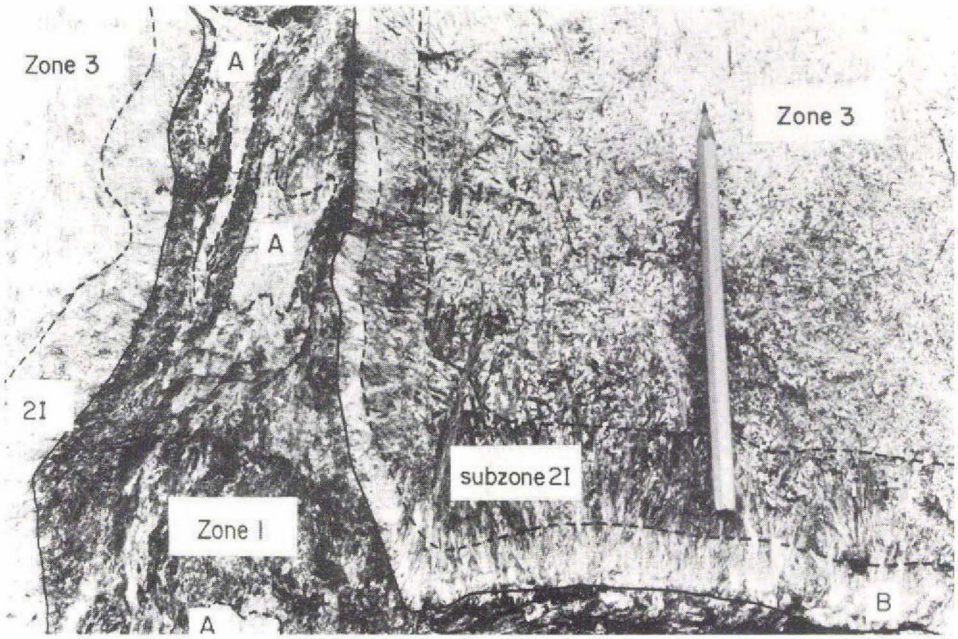

Fig. 5. Symmetrically-arranged examples of subzone 2I, which are talcose at the base (B) and which grade upward into the talc zone (zone 3).

chlorite zone and transect intermediate lithologies. The rock cuts the serpentinite in tabular sheets up to one metre thick, and these sheets display relict layering coplanar to that in the serpentinite. Euhedral crystals of carbonate comprise 25 to 45 per cent of the rock and their composition varies between $Mg_{0.6}Ca_{0.4}$ and $Mg_{0.9}Ca_{0.1}$ (by XRD), but no calcite is present. An increasing amount of serpentine occurs towards the inner contact with the serpentinite core. Magnetite veins and disseminations are common.

Serpentinite (zone 5)

The migration of ZB5 from the talc-carbonate shell into the serpentinite indicates the continual replacement of the various serpentinite phases by talc. This boundary is a weakly-defined zone, up to 0.5 m wide, where talc interfingers into the lizardite, leaving isolated enclaves of serpentine. The serpentinite rock is transected by elongate cracks which are commonly iron-stained, and the lithology preserves relic layering (fig. 9). The zone contains up to 20 per cent talc with carbonates and skeletal magnetite grains; apatite and rare chromite occur as traces.

The main serpentine phase is lizardite, which occurs as networks comprising blades and plates of interlocking grains; rare chrysotile occurs as clear and fibrous

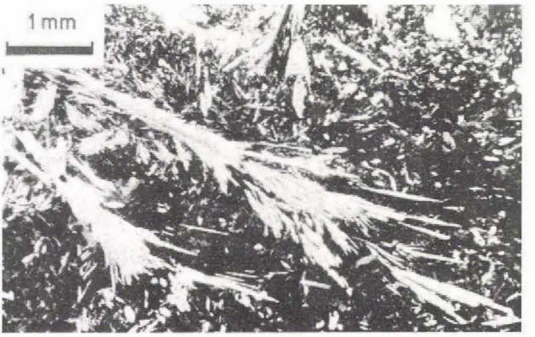

Fig. 6. Photomicrograph (X-polars) showing ferny actinolite growing perpendicular to ZB1 along a migration channel. Note the development of fine-grained tremolite-actinolite adjacent to the growths.

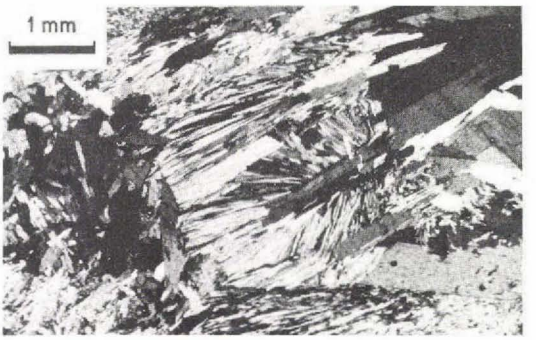

Fig. 7. Photomicrograph (X-polars) showing 'herringbone' structure, with fans of small actinolite crystals coagulating to form a more solid crystal. Note the lateral actinolites at the tips of the herringbone structures.

structures forming haloes about the carbonate crystals, and in veins. Patches lacking carbonate correspond to masses of web-like antigorite. These serpentine polymorphs were determined by the methods of Faust & Fahey (1962), Basta & Abdel Kader (1969), McKenzie (1970), Coleman & Keith (1971) and Wicks & Whittaker (1975). Carbonate is synchronous with second-phase chrysotile and is cut by chrysotile veinlets. Magnetite, defining relic layering, appears to have acted as a nucleation centre for carbonate growth.

Veins

A variety of veins cut the lens. From old to young they are: magnetite, chrysotile + asbestos, talc + dolomite, chlorite, magnesite + talc + chlorite + magnetite and talc + pyrophyllite.

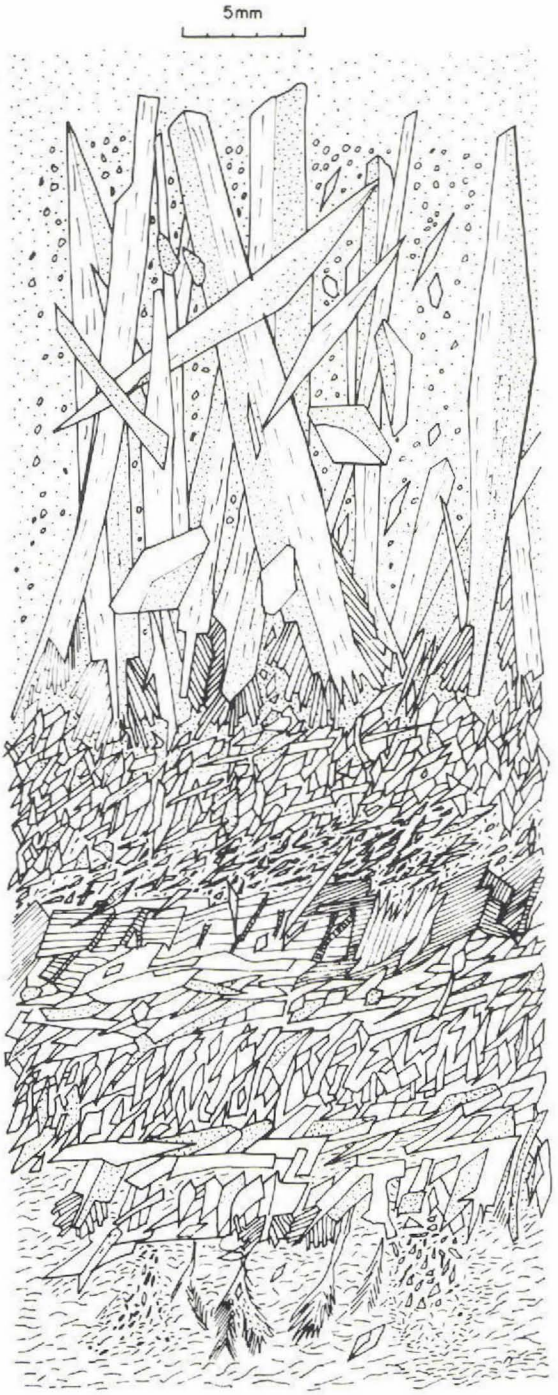

DETAIL	MAIN ZONE
XV	3
XIV	2D
XIII	2C
XII	2C
XI	2C
X	2B
IX	2B
VIII	2A
VII	2A
VI	2A
V	2A
IV	2A
III	1A/2A
II	1A
I	1A

Fig. 8. (Opposite) Illustration of the fine-scale inter-subzone boundaries from the amphibole zone which give a detailed insight into the process of mineral development. As the best defined sequence of subzones is in the amphibole zone, this has been selected for illustration.

I. The chlorite zone is a lepidoblastic intergrowth of 93 per cent chlorite with 4 per cent magnetite and a little rutile and tremolite; the accessories comprise talc, apatite, zircon and sphene.

II. The appearance of small actinolite prisms within a millimetre of the boundary is the first change in the sequence, associated with ferny amphibole clusters which overgrow early chlorite (fig. 6). Projection of migration channels also expanded the amphibole zone at the expense of chlorite, which was reduced in grain size.

III. A small extension of 'herringbone' tremolite (fig. 7) into II is associated with the development of blocky hornblende prisms which are the result of

IV. The coagulation of the 'herringbone' structure into thin strips of perpendicular acicular tremolite-actinolite up to 2 mm wide. These crystals cut the hornblende and terminate rapidly into V.

V. This is a 3 mm wide zone of lateral tremolite grains up to 3 mm long, with their long axes parallel to the boundary zones, which form the migration front. This 'herringbone' tremolite-actinolite buffer sequence may be repeated up to five times in this subzone (2A).

VI. The orientation of this zone is disrupted towards the centre of the body where the tremolite grains are realigned and involved in a thin, partly 'herringbone' layer up to 2 mm wide. The zone contains a little chlorite, which disappears at the next front.

VII. This buffer zone is always present and is similar to V. It comprises actinolite + tremolite + chlorite + hornblende and forms the junction between subzones 2A & 2B of the amphibole zone.

VIII. The interzone boundary is commonly marked by extensive growth of a chlorite intermediate between pennine and sheridanite (XRD): the chlorite books contain actinolite prisms and are commonly eaten into by tremolite veins.

IX. Later, acicular actinolites cross the front into the subzone 2A–2B boundary layer. Grains of chlorite attain a greater dimension on the inside of the zone and may be kinked, they are attacked by amphibole growths.

X. This is the transition zone between subzones 2B & 2C; the boundary relations are fairly diffuse, with a gradual coagulation of scattered and 'herringbone' actinolite domains.

XI. The combination of these micrograins gives rise to a well-defined lateral actinolite layer with 1 mm crystals. The junction with the following zone XII is rather sharp.

XII. Actinolite crystals of this zone generally form a confused jumble, with the dominant orientation perpendicular to the boundary. The system of perpendicular micrograins may occasionally lose their orientation, and develop as a felted mass. This sector gives way to XIII over 1–2 mm with an irregular boundary.

XIII. This is a coarser version of XII with tremolite-actinolite intergrowths cutting the early chlorite grains. In this zone the base of the acicular actinolite metacrysts occurs, and all minerals are attacked by talc. Local crystals of calcite and dolomite in association with magnetite, apatite, zircon and rare sphene complete the assemblage. Some large, acicular actinolites cut the mass.

XIV. The outer termination of the acicular actinolites of subzone 2D is in contact with a mass of chlorite and actinolite, whilst the other termination with ZB3 is attacked by talc. Crystals of tremolite-actinolite and hornblende at the 'bases' of the columnar actinolites are oriented with their long axes parallel or sub-parallel to the boundary.

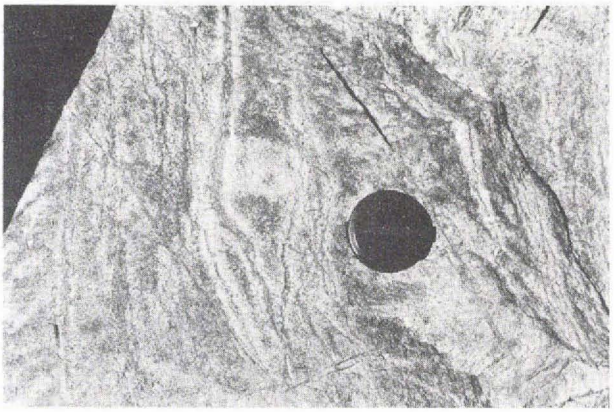

Fig. 9. Relic layering in the Ikátoq serpentinite defined by concentrations of magnetite and rare carbonate. Camera lens cap is 54 mm diameter.

Rock chemistry

Twenty samples of gneiss were analysed from the enveloping material. Of these, eight were adjacent to the contact and the remainder were collected randomly up to 100 m from the lens, to be used as a control set. The samples from the ultramafic lens consisted of: chlorite zone (7), amphibole zone (13), talc zone (1), talc-carbonate zone (2) and serpentinite zone (5). The mean zone compositions were determined by weighting the respective subzone analyses in relation to their measured width within each of the five main zones (table 2).

Gneisses

The variation in whole-rock chemistry with distance from the lens could not be determined with so few samples because of the great lithological variation in the gneisses. The main use of the analyses was in the calculation of rock formulas for the gneisses adjacent to the contact and a mean formula for those at a distance.

Ultramafic lens

The zones plot in separate fields on triangular diagrams (fig. 10) as expected from their markedly different assemblages. It is appropriate to note the interrelationships between firstly the subzones and secondly the mean zone fields as expressed on these diagrams. In both F–C–M and *fm–si–c* diagrams, the various members of the amphibole zone plot in a well-defined field which extends towards the magnesian apex with increasing talc in the subzone. Relative enrichment of Fe is evident in the chlorite zone, and the talc-carbonate and serpentinite zones plot towards the Mg apex. This field separation shows the evident concentration of Fe at the gneiss-zone 1 contact, Ca in the amphibole zone and the excess of Mg

Table 2. Chemical analyses of the main zones, calculated from subzone analyses weighted with regard to their proportional widths in the zones (F of table 1)

Analytical method: XRFS

Wt. %	Gneisses (outside)	Gneisses (Border)	Chlorite (Zone 1)	Amphibole (Zone 2)	Talc (Zone 3)	Talc-cbt (Zone 4)	Serpentinite (Zone 5)
SiO_2	66.44	61.92	39.92	49.44	48.58	49.66	37.54
TiO_2	0.53	0.59	0.38	0.09	0.07	0.05	0.03
Al_2O_3	15.69	15.52	12.34	5.82	4.86	1.78	1.55
Fe_2O_3	4.06	6.24	11.72	7.95	6.53	6.16	9.80
MgO	2.29	3.59	26.02	26.00	28.57	32.81	36.24
CaO	4.84	5.54	4.23	6.98	7.70	1.36	3.05
Na_2O	4.61	4.59	0.23	0.30	0.20	0.10	0.00
K_2O	1.25	1.39	0.12	0.06	0.06	0.04	0.00
	99.61	99.36	92.92	96.64	93.59	91.97	88.22
l.o.i.			7.08	2.35	5.66	7.59	11.46
Zr (ppm)	234	236	139	15	20	0	0
Sr "	404	277	2	1	0	0	0
Ni "	89	93	1405	3931	1198	4508	5700
Ce "	66	51	43	31	28	25	23
La "	30	18	5	5	1	2	3

l.o.i. = loss on ignition

denoted by serpentinite in the centre sections. The amphibole-zone rocks, being derived from a Ca-poor serpentinite parent in conjunction with a Ca-rich gneiss parent, suggest substantive inputs of Ca ion from an external source, or alternatively that the serpentinisation was incomplete prior to steatisation. The high modal proportion of clinozoisite in the local gneisses also indicates high Ca mobility.

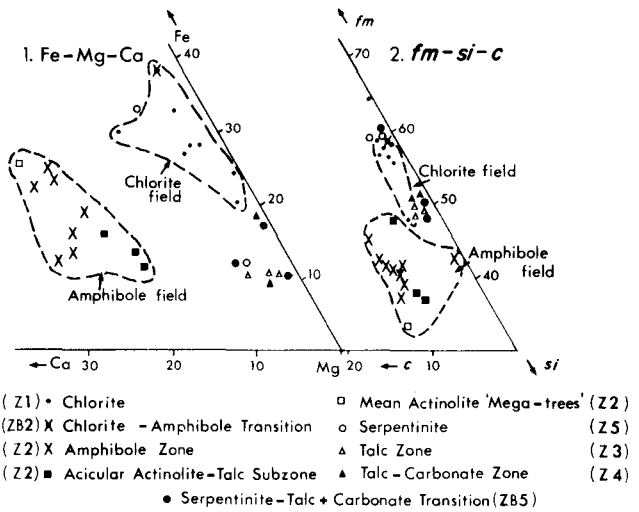

Fig. 10. Ternary Fe-Mg-Ca and Niggli *fm-si-c* diagrams to show the chemical interrelationships within the Ikátoq zoned ultramafic lens.

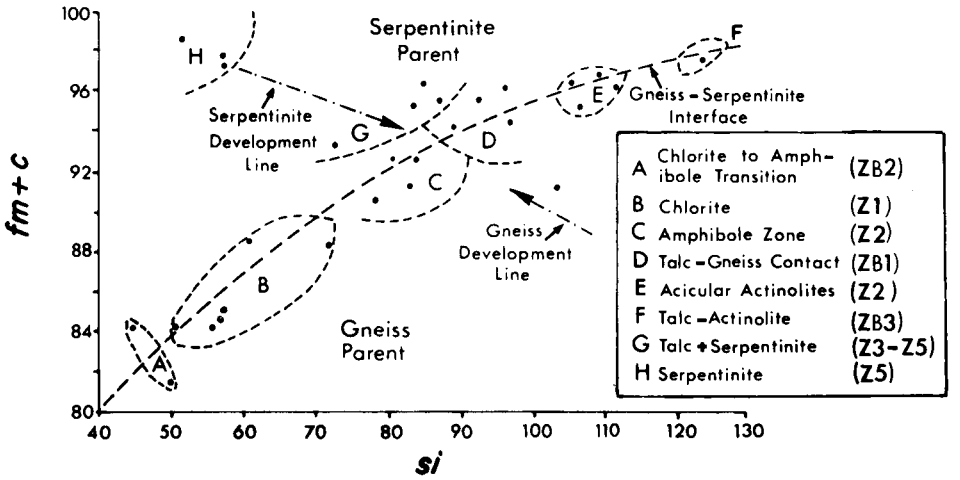

Fig. 11. Niggli (*fm* + *c*) vs *si* diagram to show the interrelationships between the zones and the original parent rocks on progressive metasomatism.

Figure 11 shows the chemical development of the serpentinite lens during progressive steatisation. The serpentinite and gneiss parent rocks are juxtaposed along their mutual reaction plane which, from this diagram, comprises the chlorite and amphibole zones. The gneiss development line indicates continuous depletion in *si* with a concomitant increase in *fm* + *c* towards the contact from the unaltered parent gneiss into the bordering gneisses: this is reflected mineralogically by the increase in clinozoisite and chlorite proportions as the contact is approached from the outside. Simultaneous alteration of the serpentinite gave rise to the talc rocks, which meet the expanded development of the original lithological junction along the 'interface line' (AF). The chlorite zone, amphibole zone and some talc subzones fall along this line with progressive alteration from chlorite-bearing to actinolite-bearing rocks towards both increasing *fm* + *c* and *si* at the expense of alkalis and other components. This suggests that the initial boundary configuration lies now within the area of the chlorite-amphibole zone boundary.

Variations across the contact between lens and gneiss

The zonal system was formed by variations in the concentrations of Si, Al, Fe, Mg, Ca and CO_2 in addition to an excess of H_2O. The selective movement of these elements is important in the generation and stabilisation of the zones, a continuing process of transfer eventually tending towards stable chlorite and talc assemblages (zones 1 and 3 respectively) as these two zones expanded at the expense of the intermediate zone now present. Curtis & Brown (1971) have followed Gibbs (1928), Thompson (1955, 1959) and Korzhinskii (1970) in the extension of the

phase rule to open rather than closed systems, and have divided the major chemical components into two main groups, actual and nonvariable. The former may be added to or subtracted from the system without altering the number of phases, the latter are interdependent on the number of phases. Mg and Fe are defined as being actual components and they maintain smooth concentration profiles between the two parent lithologies (fig. 12). Addition of nonvariable components such as Si, Al, Ca, K and CO_2 gives rise to actinolite, carbonate, chlorite and talc. The trace elements are also actual and their profiles show continuous variation due to diffusion and migration, illustrating the rapid concentration changes induced by reaction at the contact of the lens. The concentrations of Ce, La and Zr – high in the

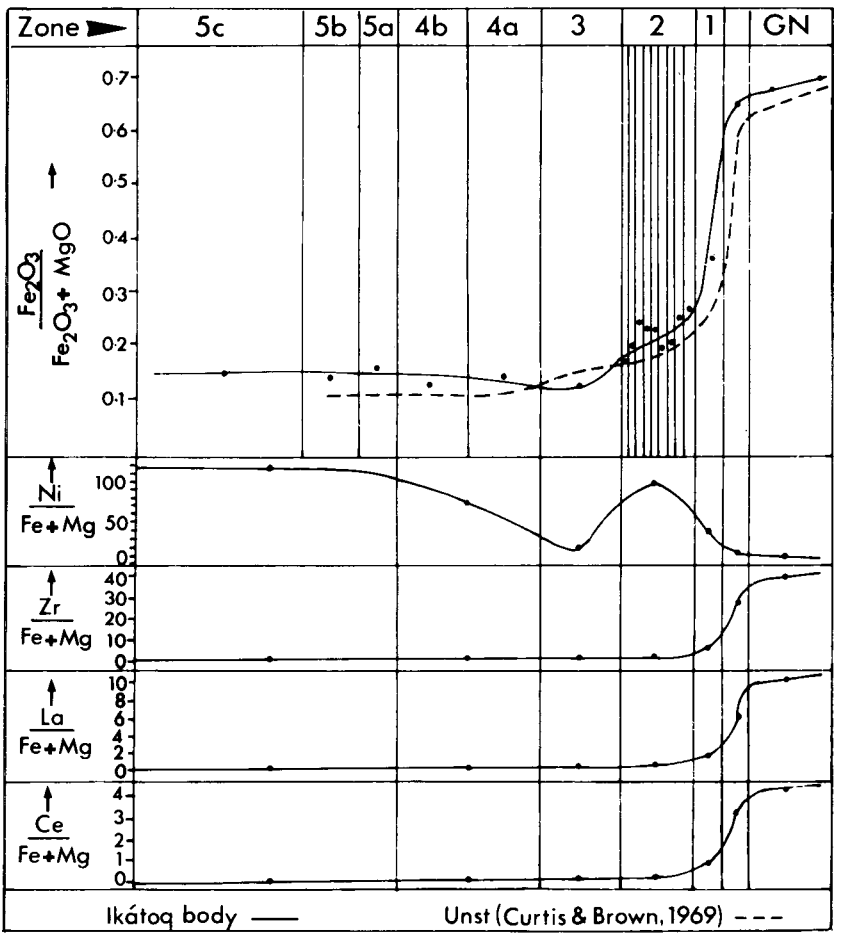

Fig. 12. Fe/Mg and trace element profiles across the contact between the gneiss and the Ikátoq zoned lens.

gneisses – drop to zero within the outer amphibole zone. The Ni profile shows a sharp drop from the lens to the gneiss at this position, indicating that the position of the original contact is somewhere within the amphibole zone.

It is beyond the scope of this paper to discuss the nature of serpentinisation; a thorough review is put forward by Moody (1976). Any arguments regarding the origin of the ultramafic parent and subsequent serpentinisation are speculative and have been omitted.

The sequential occurrence of gneiss, chlorite, amphibole and talc in reaction between ultramafic bodies and more siliceous host is similar to that discussed in the literature (cf. Read, 1934; Chidester, 1962; Jahns, 1967; Mathews, 1967; Curtis & Brown, 1969, 1971). These mineralogical zones are formed by the selective movements of ionic components migrating at different rates by a combination of pore-solution transport and ion diffusion, influenced by activity gradients set up at the contact of the two compositionally distinct materials. The migrating ions were concentrated into zones according to the principles of the theory of zoning (Korzhinskii, 1970; Weare *et al.,* 1976). These zones widened with time at the expense of both original rock bodies, and the zone boundaries (ZB1 to ZB4) moved out at different rates but never overlapped one another unless a breakdown in the migration pattern occurred (fig. 5). The establishment of local equilibrium was the main factor in the attainment of this form, and because of the differential mobility rates of the components involved in the changes, extensive material transference occurred. The zones and their subzones remained approximately constant in composition once equilibrium was established, this equilibrium being dependent on component movement rates, the chemical potentials of the perfectly mobile components of the external medium (Korzhinskii, 1970) and other thermodynamic considerations (Fisher, 1977).

Under ideal conditions of equal transfer rates for all components and constant reaction rates for all minerals, each zone boundary will be equally well-defined and sharp. However, the zone boundaries in the Ikátoq lens from ZB1 to ZB5 are characterised by a decrease in sharpness, a phenomenon expected by Korzhinskii (1970, fig. 1) and observed by Curtis & Brown (1969) in the Unst bodies. These transfer rates have been considered in some detail by Thompson (1975). Ideally the number of mineral phases within each zone should increase inwards from the outer boundary when the whole lens tends towards local equilibrium, but with time and with expansion of the monomineralic chlorite and talc zones, the reaction would reach the final equilibrium configuration with complete talcisation of the lens.

Field evidence for large scale volume change is absent, although the kink-bands in the chlorite zone attest to some movement during alteration. The layering, however, remained undeformed. Volume is an equilibrium factor during steatisation, the effect of this factor being manifested by the production of sufficient 'mobile' mineral to fill the space left by the exit of other phases such that no

concentration occurs. There is no such mineral in the Ikátoq body, with the possible exception of the carbonates, which meets this description. The gross mineralogy therefore suggests that volume contraction, probably on a minor scale, occurred during metasomatism. These aspects are considered further in the following section.

Quantitative estimations of ion migration

Field observations suggest a minor decrease in volume during steatisation. The assumption of constant volume exchange was tested using the method of Thompson (1975, p. 331) where components required to produce the bulk composition of the zoned lens from the two parent materials are tested two at a time. Thompson's example implies volume losses of about 50 per cent during the process. In the Ikátoq example, however, the volume changes implied by the test are always negative, but vary from –0.09 to –129 per cent (table 3). Results involving Ca and Al, gneiss-derived components, suggest large contractions, but these elements, specifically Ca, have been shown to be mobile at great distances from the lens. Additionally, a calculation was performed using total molar volumes, calculated from the shell volumes and densities and the mean zone compositions (table 4). Assuming that the original contact lay somewhere in the amphibole zone (fig. 11), the calculations indicate that the gross volume change during the process was of slight shrinkage (viz. 3.12 per cent) and that the constant volume calculations are a good enough approximation.

Assuming a constant-volume process of steatisation, relative mass gains and losses between zones and the two parents may be obtained quantitatively by use of the 'Modified Standard Cell' (MSC) of Barth (1952, p. 82–85) and Chidester

Table 3. Ratios of gneiss and serpentinite needed to form the present zonal thickness of 1.75 m calculated for various component pairs

Ratio	Thickness required (m) GNEISS	SERPENTINITE	Volume change (%)
Ca : Mg	1.76	1.96	- 53
Ca : Al	0.28	3.96	- 48
FMO : Ca	2.87	1.14	-129
Mg : Al	1.43	1.36	- 37
Si : Mg	0.51	1.52	- 0.1
Si : Fe	0.77	0.92	+ 0.03

FMO = FeO + MgO after the method of Thompson (1975)

Table 4. Mass balance of oxide components at constant volume

Total moles ($\times 10^3$) in all shells, normalised to R.D. = 2.65 (serpentinite-derived) and R.D. = 2.70 (gneiss-derived)

	Gneisses	Chlorite (Zone 1)		Amphibole (Zone 2)		Talc (Zone 3)	Talc-cbt (Zone 4)	Serpentinite (Zone 5)
Volume (m^3)	9.164×10^2	1.179×10^2		7.985×10^2		1.264×10^3	1.313×10^3	3.934×10^3
R.D. (F)	2.70 (1.00)	2.80 (1.04)	(1.13)	3.05	(1.15)	2.75 (1.04)	2.82 (1.06)	2.65 (1.00)
SiO_2	3659	269	2372		2372	3690	3918	8874
TiO_2	39	4	6		6	7	5	9
Al_2O_3	1466	147	474		474	626	238	622
Fe_2O_3	594	221	1014		1014	1318	1292	6157
MgO	85	124	837		837	1456	1737	5748
CaO	249	28	313		313	546	100	673
Na_2O	262	2	15		15	16	8	0
K_2O	108	1	5		5	7	5	0
l.o.i.	0	15	34		34	129	180	812
	6462	811	5070		5070	7795	7483	22895
X(F) ...		843	5729		5831	8107	7932	
Final moles	6462	Zones 1 & 2 =6572			Zones 2, 3 & 4 = 21870			22895

Σ PARENTS = 29357 : Σ PRODUCTS = 28442 (-3.12%)

Volumes calculated by integral technique for general ellipsoid from values of table 1, densities calculated from modes (table 1). Zone 1 from gneiss, 3 & 4 from serpentinite, 2 from either parent. R.D.=density, l.o.i.taken as H_2O^+

Table 5. Rock formulas of the main zones calculated according to the methods of Chidester (1962)

	Gneisses (outside)	Gneisses (Border)	Chlorite (Zone 1)	Amphibole (Zone 2)	Talc (Zone 3)	Talc-cbt (Zone 4)	Serpentinite (Zone 5)
Si	147.56	141.24	78.35	106.88	98.49	110.41	77.10
Ti	0.86	1.00	0.63	0.16	0.11	0.09	0.06
Al	15.42	15.95	10.70	5.57	4.36	1.75	1.41
Fe	2.56	4.02	6.49	4.86	3.74	3.87	5.68
Mg	3.79	6.10	38.06	41.88	43.16	54.35	55.46
Ca	5.76	6.77	4.45	8.09	8.36	3.66	3.35
Na	2.48	2.54	0.11	0.16	0.10	0.06	0.01
K	1.17	0.48	0.10	0.06	0.05	0.03	0.01
OH	0.00	0.00	11.78	4.97	8.46	12.07	18.85
O	174.32	169.86	135.37	146.37	138.97	139.09	120.86
CO_2	0.00	0.00	0.00	0.56	1.75	2.92	1.36
Total (-O)	179.60	178.10	150.67	173.19	168.58	189.23	163.27
Oeq	174.32	169.86	160.47	155.13	156.27	162.29	158.27
Cation total	100.02	98.55	99.98	100.00	99.54	101.76	100.01
Frk	1.0305	1.0486	0.9385	1.1113	1.0787	1.1659	1.0280

CO_2 was estimated from the modal carbonate content. Oeq = oxygen equivalent, Frk = cell factor

(1962). The chemical analyses obtained by the manipulation of the subzone analyses together with addition of estimated CO_2 from the modal carbonate content and H_2O from the loss on ignition were recast to give the rock formula per MSC of each of the five zones (table 5) and combined in such a way that the gains and losses per zone of the serpentinite and gneiss parent rocks could be calculated (fig. 13). It shows how the chlorite zone, considered with respect to the two parent materials, has a different nature to both, and that the major differences between the albite-enriched zone in the gneisses and the zones in the serpentinite lens lie essentially between ZB1 and ZB2 and that the amphibole zone forms a gradational contact between the chlorite zone and the serpentinite-talc body proper, thus confirming figure 12.

Calculations were made which involved the present lens dimensions and hence the quantitative shift of components during steatisation, thus giving a further estimate of volume change. 'Equivalent volumes' were computed for each zone using the modal analysis and the mineralogical 'equivalent volumes' listed by Chidester

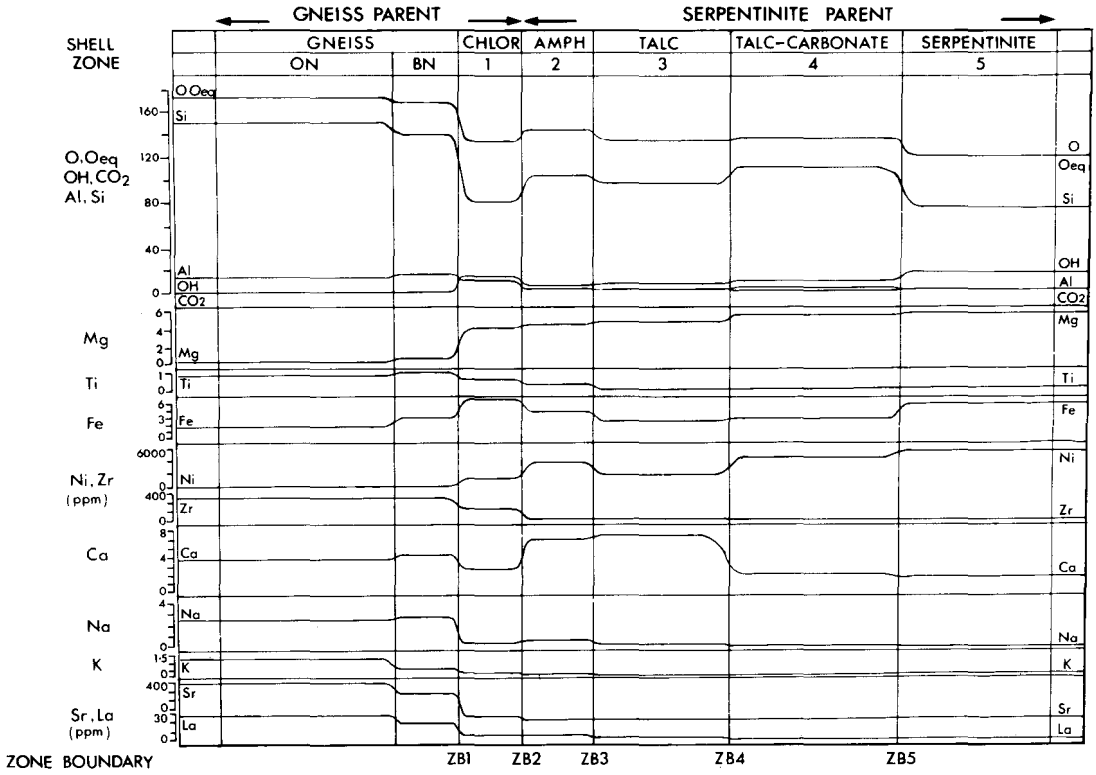

Fig. 13. Variation diagram to show mass gains and losses of the zones during steatisation, based on the rock formulae of table 5. Oeq (oxygen equivalent), O (oxygen) and OH (Hydroxyl) are calculated according to the methods of Chidester (1962). ON = outside gneiss, BN = bordering gneiss.

Table 6. Equivalent volume factors for the zones

Zone		Volume (m^3)	Equivalent volume	Equivalent volume factor	Volume (%)
Parent serpentinite		?5.794 x 10^3	20.26	1.114 x 10^5	100.00
Chlorite	(1)	0.118 x 10^3	21.34	0.025 x 10^5	2.38
Amphibole	(2)	0.799 x 10^3	18.73	0.150 x 10^5	14.14
Talc	(3)	1.264 x 10^3	19.19	0.243 x 10^5	22.93
Talc-cbt	(4)	1.313 x 10^3	17.97	0.234 x 10^5	22.10
Serpentinite	(5)	2.005 x 10^3	20.26	0.407 x 10^5	38.45
Total		5.498 x 10^3		1.057 x 10^5	100.00

Volume contraction = 5.12 per cent

(1962, p. 131). Multiplying these values by the volume of their respective shells, calculated using an integral technique for a general ellipsoid, gave an 'equivalent volume factor', E_q, for each zone (table 6). Assuming the lens to be originally serpentinite, the total E_q would have been 1.114×10^5, the present difference representing a volume contraction of 5.12 per cent – a value which agrees well with that of 3.12 per cent calculated from the molar volumes (table 4). These values are illustrated in figure 14. Adjustment of the gains and losses shown in figure 13 with regard to the present release volumes gives rise to the following mass-balanced equations using rock formulas (table 7).

In consideration of aqueous species concentrations and pH it is necessary to consider mass-balanced and energy-balanced equilibrium expressions together and solve the equations simultaneously (Helgeson, 1970). This treatment, however, is outside the scope of this paper. The mass-balanced equations of table 7 are used in the variation diagram (fig. 15). High Si values in the main zones indicate that

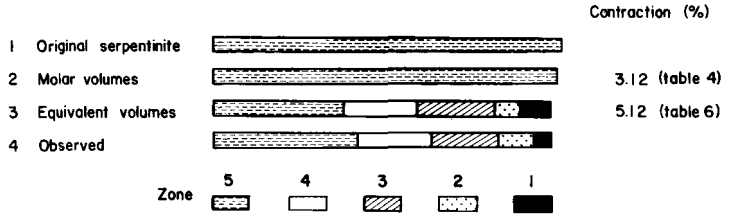

Fig. 14. System dimensions – original, observed and calculated. The percentage of the volume is represented by linear tabulation.

Table 7. Mass balanced equations for zonal changes using rock formulas

1. SERPENTINITE TO TALC CARBONATE (→ Zone 4)

   7.05 x (serpentinite formula + I) + 135.26 Si + 58 OH^- + 6.34 CO_2

   2.33 x (talc-carbonate formula) + 4.5 Mg + 73H^+

2. SERPENTINITE TO TALC (→ Zone 3)

   7.05 x (serpentinite formula + I) + 86.86 Si + 48 OH^- + 1.58 CO_2

   2.43 x (talc formula) + 30 Mg + 73H^+

3. SERPENTINITE TO AMPHIBOLE (→ Zone 2)

   7.05 x (serpentinite formula + I) + 120.90 Si + 42 OH^-

   1.50 x (amphibole formula) + 26 Mg + 58H^+ + 2CO_2

4. SERPENTINITE TO CHLORITE (→ Zone 1)

   7.05 x (serpentinite formula + I) + 5.16 Si + 90H^-

   0.25 x (chlorite formula) + 3.4 Mg + 107 H^+ + 0.2CO_2

I = metal ions (other than Si and Mg) in the reaction

---

extensive mobilisation of this component occurred during the reaction and that it concentrated in the zones most strongly altered from the serpentinite parent (talc-carbonate, talc and amphibole). The increase in Mg concentration towards the outer portions of the lens is indicative of the developing talc and amphibole zones.

If one uses ideal mineral formulas instead of rock formulas (Curtis & Brown, 1969), a volume contraction of 9.35 per cent can be calculated. This method is, however, much less accurate than using rock formulas based on bulk rock analyses. An average contraction of 5.9 per cent may therefore be obtained from the three methods.

Positional relative 'concentrations' of the components have been estimated (table 8) using the method of Curtis & Brown (1969), constructing a distance-'concentration' diagram to give a qualitative estimate of the relative activities of the various components within each zone (fig. 16). The shapes and general trends of these profiles correspond closely with those of Curtis & Brown (1969, fig. 4), suggesting that the environmental conditions required to trigger the reactions may have been similar in both cases.

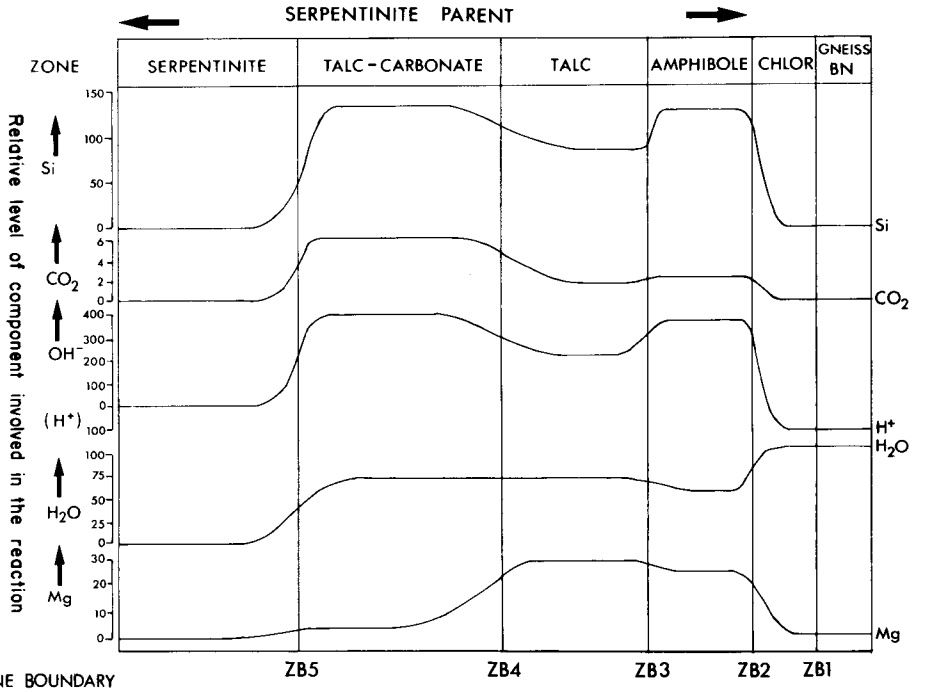

Fig. 15. Variation diagram to show the relative amount of certain components necessary to alter a zone from the parent rock, computed from equivalent volume factors in a mass-balanced system (tables 5 & 7).

Zonal Geochemistry

The relative movements of components involved in the steatisation reaction are displayed in figure 17, derived from figure 13 and the rock chemistry.

Gneiss → chlorite zone alteration

In the chlorite shell, serpentinite and then serpentinite and gneiss were converted to chlorite rock, which is considered to be primarily an alteration product of the serpentinite, later overprinted by the migration pattern created during the digestion of the gneiss envelope. The chlorite, amphibole and talc shells probably formed simultaneously; the talc development supplied Mg, Fe and H_2O to the new marginal zone. The gneisses supplied Si, Ca and some Fe to the zone along with essential Al to form chlorite and amphibole; the expulsion of Al and Na from the margin contributed to the formation of the albite-rich altered gneisses. ZB2 also

Table 8. 'Flux' estimates for zone boundaries with the slope value to be equated with component activity gradients in a qualitative sense

Boundary	Component	Mols	Mobility kg. mol. m^2	Slope	Component	Mols	Mobility kg. mol. m^2	Slope
	Si	483	3.206×10^2	3.119×10^{-3}	Mg	711	4.720×10^2	2.119×10^{-3}
Gneiss→chlorite	Al	250	1.660×10^2	6.026×10^{-3}				
Surface area (m^2) :	Ca	70	4.647×10^1	2.151×10^{-2}				
1.5064×10^3	H^+	612	4.069×10^3	2.456×10^{-4}				
(ZB1)	CO_2	40	2.655×10^1	3.766×10^{-2}				
	Si	573	3.858×10^2	2.592×10^{-3}	Mg	615	4.141×10^2	2.415×10^{-3}
Chlorite→amphibole	Al	60	4.040×10^1	2.475×10^{-2}				
Surface area (m^2) :	Ca	68	4.579×10^1	2.184×10^{-2}				
1.4852×10^3	H^+	994	6.693×10^2	1.494×10^{-3}				
(ZB2)	CO_2	40	2.693×10^1	3.713×10^{-2}				
	Si	528	3.957×10^2	2.527×10^{-3}	Mg	580	4.347×10^2	2.301×10^{-3}
Amphibole→talc	Al	30	2.248×10^1	4.448×10^{-2}				
Surface area (m^2) :	Ca	40	2.998×10^1	3.336×10^{-2}				
1.334×10^3	H^+	1070	8.019×10^2	1.247×10^{-3}				
(ZB3)	CO_2	40	2.998×10^1	3.336×10^{-2}				
	Si	339	3.149×10^2	3.176×10^{-3}	Mg	284	2.639×10^2	3.788×10^{-3}
Talc→talc-cbt	Ca	30	2.788×10^2	3.587×10^{-3}				
Surface area (m^2)	H^+	588	5.465×10^2	1.830×10^{-3}				
1.0760×10^3	CO_2	40	3.717×10^1	2.690×10^{-2}				
(ZB4)								

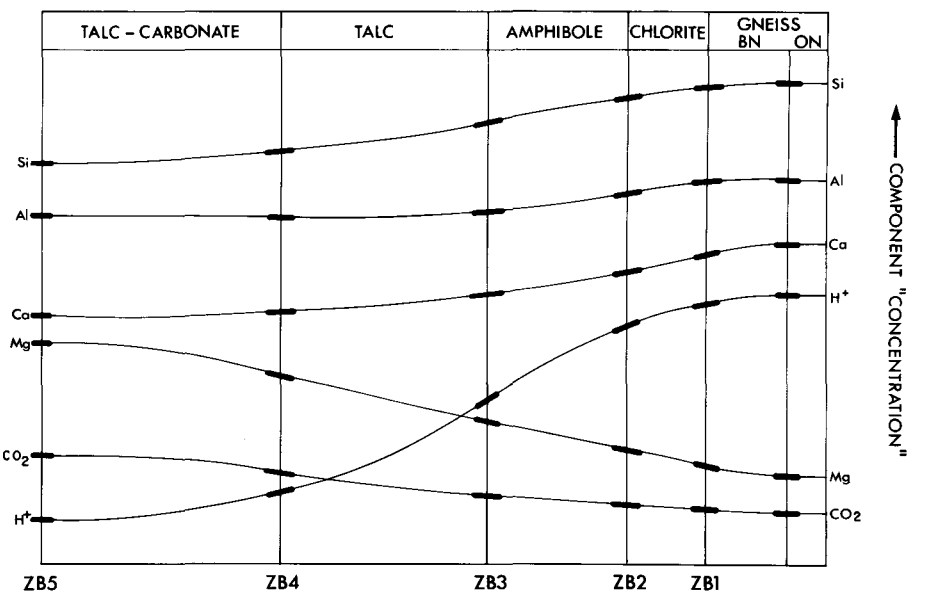

Fig. 16. Concentration profiles of various components in the steatisation reaction calculated from the 'total fluxes' (table 8) and based on Curtis & Brown (1969).

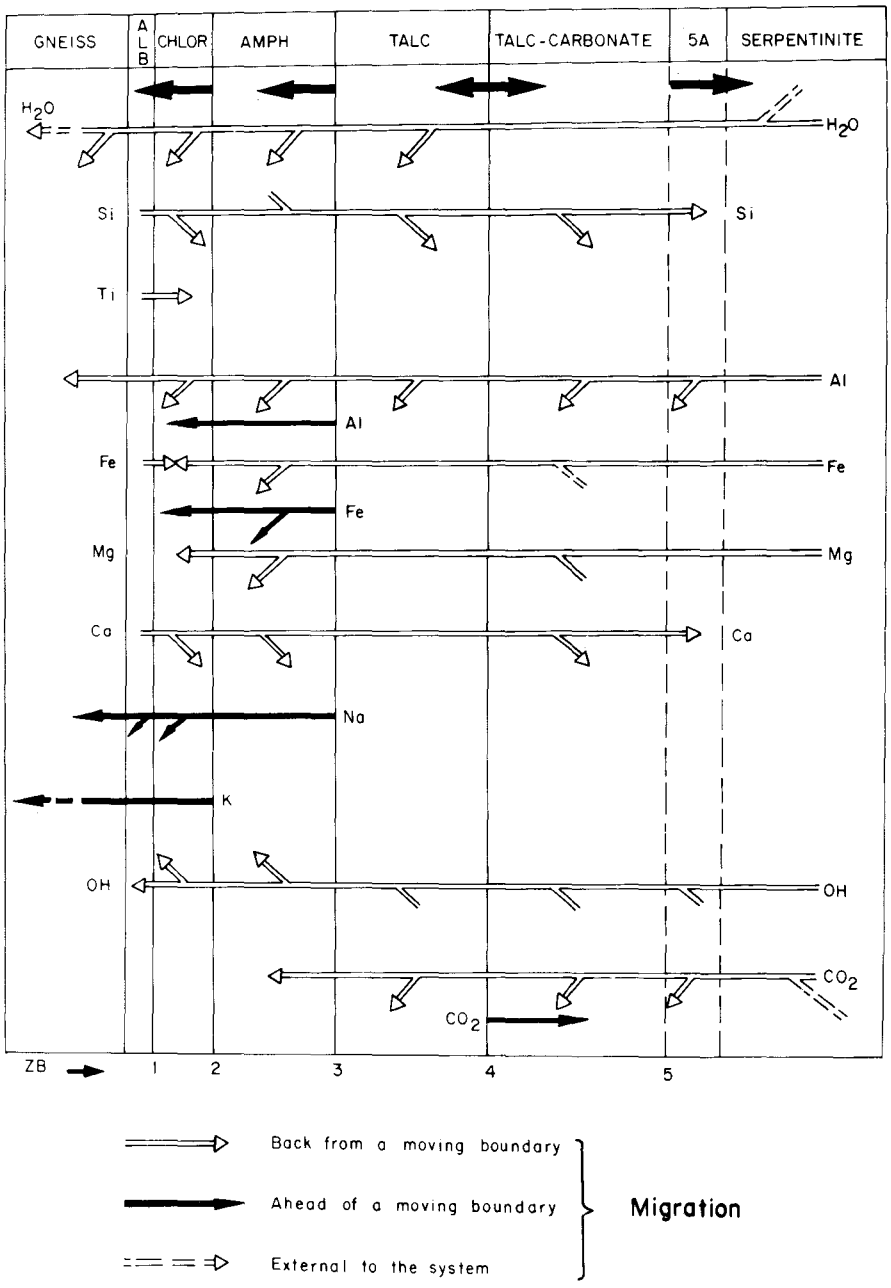

Fig. 17. Reference figure after Jahns (1967), showing the movement of the major components in the system during steatisation in a qualitative manner.

moved outward, but at a rate which resulted in steady expansion of the chlorite zone. Persistence of such phases as zircon, rutile, apatite, sphene and ilmenite into the chlorite zone is a function of their resistance to 'chloritisation'. Digestion of the chlorite and amphibole zones by the talc zone was based on the advance of ZB3, attributable to a build-up in the Si concentration. Simultaneous growth of tremolite-actinolite in the chlorite zone was due to the bi-directional migration pattern of Fe (fig. 17) and the inward migration of Al from the destruction of plagioclase in the bordering gneisses. Mg was continuously supplied to the developing chlorite and amphibole zones by transfer from the serpentinite core. Ca migrated towards the centre of the body into the developing talc and talc-carbonate zones, with permanent CO_2 excess. Some Ca was retained by subzones 2D and 2I, giving rise to a patchy distribution of carbonate. The outward migration of Mg, inward migration of Si and an increase in the partial pressure of CO_2, along with H^+ activity and continuous supply rates, produced talc at the expense of early tremolite. The tremolite acted as a Ca-sink, forming talc-tremolite rock (1B, table 1), replacing the chlorite and early tremolite. Replacement of chlorite by tremolite and then by talc is in direct contrast with the falling-temperature sequence ('amphibole'-tremolite-chlorite) proposed by Du Rietz (1935, p. 244).

Chlorite → amphibole zone alteration

The amphibole zone lies in a position where the chemical potential of Mg was insufficient to form talc and that of Fe and Al was insufficient to form chlorite. The similar concentrations of Fe and Ca in this zone compared to the chlorite zone puts this zone in the stability field of both amphibole and chlorite. A steady inwards-decrease of the carbonate content is due to a selective increase in the partial pressure of CO_2 associated with an increase in Ca activity towards ZB3. The primary reaction in the zone, the conversion of serpentinite to tremolite-actinolite, has a strong negative volume change, and assuming constant component supply, results in a volume contraction of 13 per cent.

Intimate intermixing of phases and the formation of diverse subzones in the amphibole zone is a function of the small-scale variation in the concentration and chemical potentials of Si, Al, Fe, Mg and Ca with constant H_2O and local 'highs' of Si, Ca, CO_2 and H_2O activity stabilising talc and local carbonate. Movement of Si, Fe, Mg and Ca through the zone was both by 'migration channels' along the acicular actinolites and by intergranular diffusion. Sharp, consistent replacement fronts between particular subzones indicate that the fluctuations in component concentration are due to systematic arrangements in the activity gradients; however, recalculation of the rock formulas from adjoining subzones imply that the mineralogical changes were in response to the alteration in activity of one component. In general, an alternation of the character of a component between inert and mobile results in a different assemblage. For example, the bulk compositions of

subzones 2C and 2D are approximately the same, but 2C contains abundant chlorite whilst 2D is characterised by acicular actinolites with carbonates, talc and chlorite in the matrix. Chemically, this represents an intrazone stabilisation of the dominant components Mg, Al and Ca, with high Fe activity in 2C giving way to high Si activity in 2D. Other subzone jumps, for instance 2B → 2C, involve a steady concentration of Ca, Ti and (Mg), with sharp replacement gradients involving Si, Al and Fe.

Amphibole → talc zone alteration

Alteration of the chlorite and tremolite substrate to talc by an increase in the chemical potential of Si is a dominant process adjacent to ZB3. The rocks of the talc zone advanced outwards by means of a relatively sharp replacement front (ZB3) into the amphibole zone, with a concomitant migration of ZB1 and ZB2 towards the gneiss and an almost stationary ZB4. This expansion involved mainly the addition of Si and CO_2 and the loss of H_2O at the expense of the chlorite and amphibole of the external shells.

Difficulties in the accurate placement of ZB3 have an important corollary concerning chemical aspects of boundary migration within the amphibole zone. The chemical potential of Si is generally insufficient to form talc, except within subzones 2D and 2I, where it forms interstitially to the large acicular actinolites at the expense of a decrease in the Mg activity. Across ZB3, the chemical potential of Si attains sufficient stability with Si and Mg components along the actinolites for the formation of talc. Within the talc zone, near ZB4, the partial pressure of CO_2 was sufficiently high to form scattered microcrystals of carbonate, indicative of a steep CO_2 gradient in the ZB4 area. The presence of similar microcrystals in the ZB3 area is not as simple to accommodate. The advance of ZB3 is preceded at a distance of about 20 mm by a tenuous band of carbonate-bearing talc + actinolite + chlorite rock with magnesite and dolomite rhombs overgrowing the talc mass. It may be that these crystals formed in response to a local high in the partial pressure of CO_2, which, together with Mg derived from the destruction of chlorite, formed a band uniformly parallel to the margin of the lens.

Generally, carbonate grains within the talc zone are more magnesian towards ZB4 (XRD), which may correspond with a slight increase in Fe substitution in the talc lattice.

Talc → talc-carbonate zone alteration

Talc-carbonate rock forms a distinct 'transgressive' lithology between the serpentinite and talc zones. ZB4 is diffuse, but remained stationary during metasomatism, whilst the even more indistinct ZB5 migrated into the serpentinite, resulting in a substantial expansion of the talc-bearing lithologies. The reaction for

the conversion of serpentinite to talc-rocks mainly involves the addition of CO_2 and the migratory components Ca, Mg and Fe, producing H_2O. Stoichiometry of the equation is impossible to obtain with the influence of these components and the patchy distribution of reactant and product species, specifically the irregular occurrence of dolomite or magnesite. High potentials of Ca and Mg with high CO_2 partial pressure gave rise to carbonate rhombs with formulae varying between $(Ca_{0.75}Mg_{0.25})CO_3$ and $(Ca_{0.2}Mg_{0.8})CO_3$ (XRD & XRF recalculation). ZB4 marks the point at which the chemical potential of Si declined sufficiently so that a 100 per cent talc assemblage was replaced by talc and carbonate. Volume relations in the talc–talc-carbonate system are linked with the talc zone expansion. There are no distortions of the relic layering or veins, and the textural relations indicate that replacement was on a volume-for-volume basis.

Serpentinite → talc-carbonate zone alteration

The contact relations across ZB5 into the serpentinite are diffuse and mark the furthest ingress of Si to raise the chemical potential of Si high enough to create talc. The actual position of the boundary was one at which the potential of CO_2 was sufficiently high to stabilise the formation of talc from serpentine such that talc + magnesite was the stable assemblage. Continuous Mg movement from the destruction of the serpentinite parent and autoproduction of water assisted the change. The nature of the boundary, in that it completely penetrates the serpentinite in tabular sheets, indicates the irregularity of the source regions of H_2O and CO_2 migration.

Discussion

The validity of the mass-balanced manipulations in the preceding section is supported by Fick's First Law of Diffusion, and Korzhinskii (1970, p. 111) indicates that the conditions to be satisfied for the application of this law are as follows: first, that the components must be transported through pore-solution diffusion, and secondly that the reaction must proceed with no substantial change of volume. In the case of the Ikátoq model, the mechanics of grain-boundary diffusion are not completely applicable, because the pattern was disturbed by the formation of 'migration channels', suggesting that fluid flow in certain parts of the lens may have predominated over cation diffusion in this case. Excluding these channels, the system contains features characteristic of diffusion-controlled structures (Fisher, 1977), for instance, the formation of distinct zones with sharp boundaries indicative of increased activity of certain components, which reacted to give the diagnostic minerals of these zones, was combined with zonal stabilisation due to equilibration of component activity. The former process requires circulating solutions, the

latter needs more quiescent conditions. Both may be satisfied by assuming that the steady-state conditions alternated with short pulses of H_2O and CO_2 addition, which were unable to affect the local equilibrium state to such an extent that delicate balance between reactants and products in the developing system could be interrupted. Water was certainly present in excess and was probably the main diffusive transport medium; it thus becomes valid to consider all reactions – most of which were water-producing – in the light of the ubiquitous water as a non-reactant phase.

Rapid variations in component concentration at replacement fronts (zone boundaries) which, in an ideal situation, should form very sharp zone boundaries, are to some extent blurred by lag characteristic of the different transfer rates of the components. The growth of talc and chlorite zones at the expense of the serpentine and amphibole zones may be explained by the favourable mineralogy and chemistry of these zones to accept the total migrating components. Possibly the more favourable orientation of the sheets of talc and chlorite may have given rise to an effective 'crystallisation pressure', where the two minerals grew at the expense of other, more irregularly-oriented assemblages. Thus, the essentially monomineralic chlorite and talc zones expanded, eventually to occupy the whole lens had the reaction been completed.

Conclusions

The parent of the zoned ultramafic body at Ikátoq was probably peridotitic, mobilised at high water vapour pressure. During transport, the peridotite was altered to serpentinite by a possible combination of autometamorphism and external aqueous influence; the process being completed after the body was intruded into locally ductile gneisses, possibly during local high-grade metamorphism. Steatisation was induced during the cooling period following the main metamorphism about 2850 m.y. ago, when temperatures were probably about 350°C and the lithostatic pressures were lower than the 7.5 kb typical of the main metamorphic event. The process occurred with H_2O and CO_2 excess and mobilised Ca and Na from the gneisses, which, together with the Ca excess produced by final-stage serpentinisation of the original mass, gave rise to the present display of albite- and clinozoisite-rich rocks which form an envelope about the ultramafic lens. The whole system represents a metasomatic reaction, frozen at an incomplete stage, possibly due to rapidly waning local temperatures or a cessation in the supply of H_2O and CO_2 – the essential materials for the transformation.

A concentration gradient was set up at the junction of the two compositionally-distinct original materials, which rapidly diversified under the influence of the hydrothermal fluids used as transport media, and formed a series of zones, the

metasomatic column, independent of falling temperature. Differential component transfer rates obscured the detailed interrelationships of the zones which are furthest separated from the original interface, whereas those boundaries near the contact are sharp. Mobilisation of selected components in each parent rock, serpentinite and gneiss, initiated ion migration and bulk transport, which proceeded with progressive metasomatism towards complete assimilation of both parent rocks, eventually trending towards monomineralic rocks comprising talc and chlorite respectively.

Most components required for the overall reaction were obtained from within the lens, but the surrounding gneisses supplied Al, Ca and K for the final transformation, whilst the lens gave off Mg. Water and CO_2 were totally mobile and always in excess. The lens contracted in volume by about five per cent during the reaction, although there is evidence of local expansion in the chlorite zone where chlorite books have kink-bands, and lobate fingers of chlorite cut albite porphyroblasts in the gneiss. Late veining and alteration were initiated by leaching solutions percolating along a fracture system.

Acknowledgements

I am grateful to K. Coe and B. Chadwick of the University of Exeter, England, under whose guidance this work was carried out. I thank D. Dallow for the chemical analyses, J. Saunders for the photographs and I. Taylor for his efficient thin section making. Professor G. von Gruenewaldt allowed me time to complete the paper in its present form and R. A. Hunter drafted some of the figures. The very constructive comments of the referee, H.-R. Pfeiker, Lausanne, are greatly appreciated.

The essentials of this work were carried out as part of a PhD project at the University of Exeter, financed by the Natural Environment Research Council and the Geological Survey of Greenland.

References

Barth, T. F. W. 1952: *Theoretical petrology.* New York & London: Wiley & Sons. 416 pp.

Basta, E. Z. & Abdel Kader, Z. 1969: The mineralogy of Egyptian serpentinites and talc-carbonates. *Mineralog. Mag.* **37,** 394–408.

Black, L. P., Moorbath, S., Pankhurst, R. J. & Windley, B. F. 1973: $^{207}Pb/^{206}Pb$ whole rock age of the Archaean granulite facies metamorphic event in West Greenland. *Nature* **244,** 50–53.

Chidester, A. H. 1962: Petrology and geochemistry of selected talc-bearing ultramafic rocks and adjacent country rocks in north-central Vermont. *U.S. geol. Surv. Prof. Pap.* **345,** 207 pp.

Coleman, R. G. & Keith, T. E. 1971: Serpentinisation, Burro Mountain, California. *J. Petrol.* **12,** 311–328.

Curtis, C. D. & Brown, P. E. 1969: The metasomatic development of zoned ultrabasic bodies in Unst, Shetland. *Contr. Mineral. Petrol.* **24,** 275–292.

Curtis, C. D. & Brown, P. E. 1971: Trace element behaviour in the zoned ultramafic bodies of Unst, Shetland, *Contr. Mineral. Petrol.* **31,** 87–93.

Du Rietz, T. 1935: Peridotites, serpentinites and soapstones of northern Sweden. *Geol. Fören. Stockh. Förh.* **57,** 133–260.

Faust, G. T. & Fahey, J. J. 1962: The serpentine-group minerals. *U.S. geol. Surv. Prof. Pap.* **384A**, 92 pp.

Fisher, G. W. 1977: Nonequilibrium thermodynamics in metamorphism. *In* Fraser, D. G. (edit.) *Thermodynamics in geology.* 381–403. Dordrecht, Holland: Riedel.

Gibbs, J. W. 1928: *The collected works of J. Willard Gibbs.* 1. Yale University Press. 434 pp.

Helgeson, H. C. 1970: A chemical and thermodynamic model of ore deposition in hydrothermal systems. *Mineral. Soc. Amer. Spec. Pap.* **3**, 155–186.

Jahns, H. 1967: Serpentinites of the Roxbury district, Vermont. *In* Wyllie, P. J. (edit.) *Ultramafic and related rocks.* 137–160. New York: Wiley & Son.

Korzhinskii, D. S. 1970: *Theory of metasomatic zoning.* Oxford: Clarendon Press. 158 pp.

McGregor, V. R. 1973: The early Precambrian gneisses of the Godthåbsfjord district, southern West Greenland. *Phil. Trans. Roy. Soc. Lond.* **A-273**, 343–358.

McKenzie, R. C. 1970: Simple phyllosilicates based on gibbsite- and brucite-like sheets. *In* McKenzie, R. C. (edit.) *Differential thermal analysis.* 1. 497–537. London & New York: Academic Press.

Mathews, D. W. 1967: Zoned ultrabasic bodies in the Lewisian of the Moine nappe of Skye. *Scott. J. Geol.* **3**. 19–32.

Moody, J. 1976: Serpentinisation: a review. *Lithos* **9**, 125–130.

Moorbath, S. & Pankhurst, R. J. 1976: Further rubidium-strontium age and isotopic evidence for the nature of the late Archaean plutonic event in West Greenland. *Nature* **262**, 124–126.

Read, H. H. 1934: The metamorphic geology of Unst in the Shetland Islands. *Quart. J. geol. Soc. Lond.* **90**, 637–688.

Thompson, A. B. 1975: Calc-silicate diffusion zones between marble and pelitic schist. *J. Petrol.* **16,** 314–346.

Thompson, J. B. 1955: The thermodynamic basis for the mineral facies concept. *Amer. J. Sci.* **253**, 65–103.

Thompson, J. B. 1959: Local equilibrium in metasomatic processes. *In* Abelson, P. H. (edit.) *Researches in geochemistry,* 427–457. New York: Wiley & Sons.

Weare, J. H., Stephens, J. R. & Eugster, H. P. 1976: Diffusion metasomatism and mineral reaction zones: general principles and application to feldspar alteration. *Amer. J. Sci.* **276**, 767–816.

Wells, P. R. A. 1976: Late Archaean metamorphism in the Buksefjorden region, Southwest Greenland. *Contr. Mineral. Petrol.* **56,** 229–242.

Wicks, F. J. & Whittaker, E. J. W. 1975: A reappraisal of the structures of the serpentine minerals. *Can. Mineral.* **13,** 227-243.

Windley, B. F. 1972: Regional geology of early Precambrian high-grade metamorphic rocks in West Greenland. Part 1: Kângnaitsoq to Ameralik. *Rapp. Grønlands geol. Unders.* **46**, 46 pp.

ISSN 0105–3507

AiO Tryk as, Odense